Available online at www.sciencedirect.com
SCIENCE DIRECT®
Surface Science 526 (2003) L143–L150
SURFACE SCIENCE
www.elsevier.com/locate/susc

Surface Science Letters

Driving forces for Ag-induced periodic faceting of vicinal Cu(1 1 1)

A.R. Bachmann [a,b,*], S. Speller [b], A. Mugarza [c], J.E. Ortega [c,d]

[a] Fachbereich Physik, Universität Osnabrück, Barbarastrasse 7, Osnabrück 49069, Germany
[b] Research Institute for Materials, University of Nijmegen, Toernooiveld 1, ED 6525 Nijmegen, The Netherlands
[c] Departamento de Física Aplicada I, Universidad del País Vasco, Plaza de Oñate 2, San Sebastian E-20018, Spain
[d] Donostia International Physics Center, Centro Mixto CSIC/UPV, Manuel Lardizabal 4, San Sebastian 20018, Spain

Received 24 October 2002; accepted for publication 21 November 2002

Abstract

Adsorption of submonolayer amounts of Ag on vicinal Cu(1 1 1) induces periodic faceting. The equilibrium structure is characterized by Ag-covered facets that alternate with clean Cu stripes. In the atomic scale, the driving force is the matching of Ag(1 1 1)-like packed rows with Cu(1 1 1) terraces underneath. This determines the preference for the facet orientation and the evolution of different phases as a function of coverage. Both Cu and Ag stripe widths can be varied smoothly in the 3–30 nm range by tuning Ag coverage, allowing to test theoretical predictions of elastic theories.

Keywords: Vicinal single crystal surfaces; Faceting; Copper; Silver; Scanning tunneling microscopy; Low energy electron diffraction (LEED)

Self-organization on crystal surfaces is a promising alternative for growing uniform nanostructures with regular sizes and spacings [1,2]. In the case of one-dimensional nanostructures one can use the regular step arrays of vicinal surfaces as templates. Ideally atomic steps are preferential adsorption sites, and wires and stripes can be grown by step-flow. However, if the terrace width increases to a few nanometers, single steps tend to meander and their spacing becomes irregular. Yet vicinal surfaces offer another alternative at this mesoscopic scale, i.e., using adsorbates to induce the formation of periodic facets, which are much stiffer than individual steps. In this case the miscut angle as well as the adatom concentration can be tuned to obtain a variety of stripe patterns that are potential templates for further nanostructure growth [3–7]. The fundamental problem is controlling this complex process in order to predict and obtain useful template structures. Therefore it is important to understand the microscopic mechanisms that determine the stripe pattern formation.

In lattice-matched systems, adsorbates can induce faceting into crystal planes with particularly

* Corresponding author. Address: Research Institute for Materials, University of Nijmegen, Toernooiveld 1, ED 6525 Nijmegen, The Netherlands. Tel.: +31-24-365-3093; fax: +31-24-365-2190.
E-mail address: bachmann@sci.kun.nl (A.R. Bachmann).

0039-6028/02/$ - see front matter
PII: S0039-6028(02)02574-8

low surface free energy [8]. But generally also the lateral dimensions have to be considered and the driving force is stress relieve reached by lattice matching of the adsorbate layer with a particular substrate orientation. The high step density of the vicinal surface facilitates the step bunching and the formation of facets with better lattice matching in the direction perpendicular to the steps. Thus at a temperature where both adatom and surface step mobilities are high enough the system breaks up into two phases, namely well-matched adsorbate-covered facets and adsorbate-free stepped stripes. A widely studied case is Au on vicinal Si (v-Si). Here a variety of overlayer reconstructions match to different Si crystal planes, leading to a family of striped patterns made of low symmetry facets and wide (1 1 1) or (1 0 0) terraces with different Au concentrations [3–5]. The final morphology depends on the total amount of Au deposited, the temperature and the vicinal angle of the clean surface. Furthermore, one can tune miscut angle and Au coverage to obtain a well-matched single phase system [4]. More recently adsorbate-induced faceting and nanostructuration has been observed for Ag and NaCl on v-Cu(1 1 1) [6,7]. In these cases the lattice matching is good between Ag(1 1 1) and Na(1 0 0) packed layers and Cu(1 1 2) and Cu(2 2 3) planes, respectively. This induces stripe patterns of covered and uncovered facets, as well as changes in the facet orientation as a function of coverage.

The important question concerns the mesoscopic scale, i.e. the nanostructure periodicity. Using the elastic theory of continuous media for two-phase systems Marchenko has shown that the difference in stress energy between the two phases produces long-range interactions, leading to periodic domain patterns [9]. Although this theory explains well the spontaneous faceting of clean surfaces [10] or the coverage-dependent periodicity of adsorbate patterns on flat surfaces [11], it is an open question whether it can be applied for adsorbate-induced faceting. On the one hand, because the growth of strained layers might bring in other types of elastic relaxations, thereby suppressing the characteristic wavelength [12]. On the other hand, the adsorbate-induced faceting is a more complex process that involves huge mass transport and restructuration of two different chemical species, and hence it is more likely to be kinetically restricted. This is the case of Au/v-Si(1 0 0) and NaCl/v-Cu(1 1 1) [7,13]. Here we analyze the Ag-induced faceting of v-Cu(1 1 1). We show that this self-assembled striped structure can be tuned in the 3–30 nm range by simply controlling Ag coverage. [1] The morphology of the system is stable over a wide temperature range. At the atomic scale we show that faceting is driven by the tendency of Ag to form (1 1 1)-like packed layers with minimum strain. At the mesoscopic scale we are able of proving, for the first time in adsorbate-induced faceting, the coverage-dependent periodicity predicted by the continuum elastic theory at thermal equilibrium.

The substrate is v-Cu(1 1 1) with 11.8° miscut about the $[\bar{1}\,\bar{1}\,2]$ direction, close to Cu(2 2 3) which has nominally a 11.4° miscut. The surface preparation is described elsewhere [6]. Ag deposition was done with the substrate held at 300 K. The regular stripe structure is produced after subsequent annealing to 420 K. Further annealing to 700 K does not produce any appreciable change in scanning tunneling microscopy (STM) images or low energy electron diffraction (LEED) patterns, strongly suggesting thermal equilibrium. In order to have a continuous variation of the coverage, Ag is deposited as a wedge. The coverage is calculated from STM images using 3000 $\mathring{A}^2$ frames and assuming that Ag covered areas consist of packed, 1 monolayer (ML) thick patches. Such assumption is consistent with the structural analysis of Ag-covered areas and also with Auger electron spectrocopy measurements [6].

In Fig. 1(a)–(e) we study the morphology of the system as a function of Ag coverage by means of STM and LEED. Fig. 2 schematically depicts the side view of the faceted structure deduced from the analysis. The clean surface shows a regular array of monoatomic, {1 0 0}-like steps along the $[\bar{1}\,1\,0]$ direction, giving rise to the characteristic spot splitting in LEED [14]. The average terrace width measured with both LEED and STM is $d = 10.2$

[1] This makes Ag/Cu system very attractive to tailor surface states [15].

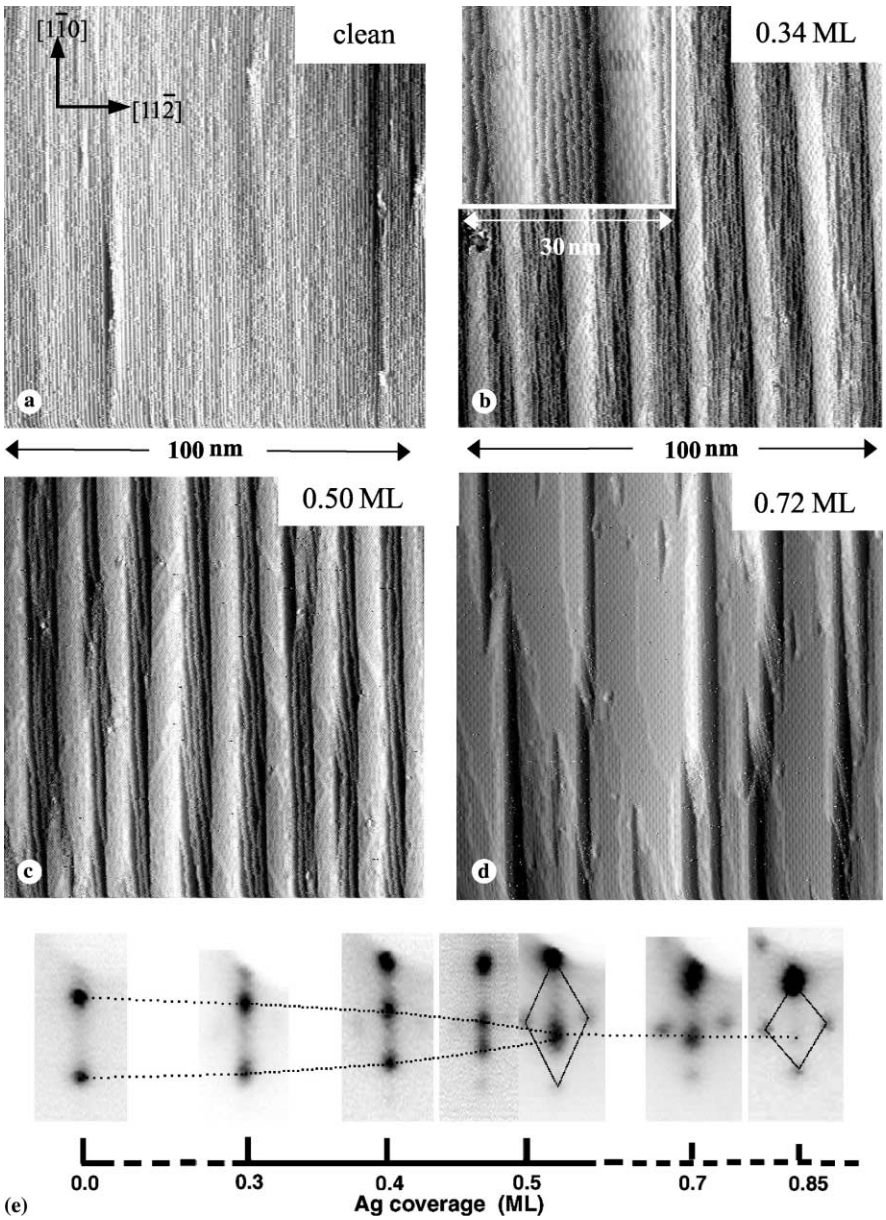

Fig. 1. (a)–(d) STM images and (e) (0, 0) LEED spot measured at different coverages for Ag-induced faceting in vicinal Cu(1 1 1). Up to 0.6 ML, the system displays periodic, two-phase separation of Ag-covered (1 1 2) facets and clean Cu stepped stripes. Both give distinct LEED structures in (e), i.e., spot splitting for Cu stripes (marked by the dotted lines) and Moiree pattern spots for Ag facets (indicated by rhombuses). As the Ag coverage increases from (a) to (c), steps from Cu stripes incorporate in Ag facets, such that Cu terraces become wider. This is proved by the splitting reduction in (e). (3 3 5) facets like those in (d) develop beyond 0.6 ML.

Å, i.e., the surface mostly shows (2 2 3)-like terraces ($4\frac{2}{3}$ atomic rows per terrace, $d = 10.5$ Å) with a few (3 3 5)-like terraces ($3\frac{2}{3}$ atomic rows, $d = 8.4$ Å). As shown in Fig. 1(b)–(d), upon Ag adsorption

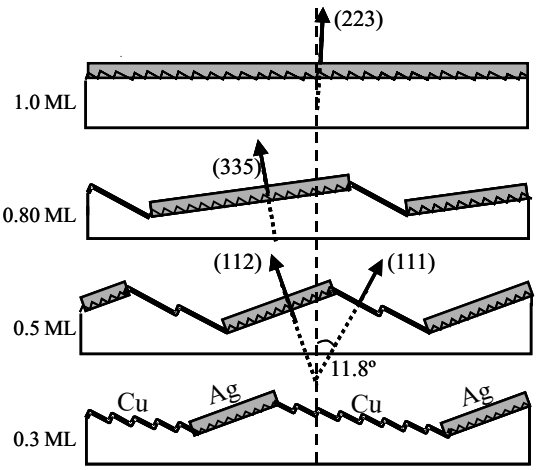

Fig. 2. Schematic evolution of the periodic faceting induced by Ag on vicinal Cu(1 1 1) with 11.8° miscut, as deduced from the STM-LEED analysis in Fig. 1.

the system undergoes faceting. Below 1 ML we distinguish three different regimes, which differ on the crystallographic orientation of the Ag-covered facet. These are the *A*-regime up to ~0.52 ML, the *B*-regime between ~0.52 and ~0.76 ML, and the *C*-regime from ~0.76 to 1 ML.

Fig. 1(b) and (c) correspond to the *A*-regime, which is characterized by a fairly regular hill-and-valley structure of Ag-covered facets oriented in the (1 1 2) direction and clean Cu stepped areas. The inset of Fig. 1(b) shows a closer view of the surface, where we can observe the Moire pattern in the Ag-covered facet, and monoatomic steps at clean Cu stripes with their typical frizzy edges. In the LEED pattern we have both the spot structure from the Ag Moire and the splitting from the step array in the Cu stripe. As observed in Fig. 2(b) and (c) and depicted in Fig. 2, increasing the Ag coverage in *A*-regime results in a higher density of Ag-covered stripes and a reduction of the step density at clean Cu bands. The latter is due to the fact that Cu(1 1 2) facets ($d = 6.25$ Å, $2\frac{2}{3}$ atomic rows per terrace) have higher step density than the average surface, thus their relative growth requires additional steps from Cu stripes. Such effective step removal from Cu stripes is nicely followed in the LEED pattern in Fig. 1(e). The Cu splitting smoothly shrinks as a function of Ag coverage, and both spots merge into a single one with 0.52 ML, when *A*-regime saturates. [2]

The *B*-regime from 0.52 to 0.76 ML is characterized by a smooth transition in the Ag-covered facet orientation from (1 1 2) to (3 3 5). The latter is closer to the surface normal, allowing a higher Ag saturation. (3 3 5)-covered areas develop directly from the center of preexisting (1 1 2) facets or arise by melting two contiguous (1 1 2) facets. In both cases, the (3 3 5) orientation characterizes the center of the Ag-covered stripes, whereas the boundaries preserve the (1 1 2) orientation. For 0.72 ML in Fig. 1(d) the *B*-regime is almost saturated, i.e., we have flat Cu(1 1 1) terraces and mostly (3 3 5)-oriented Ag stripes, also displaying a Moire structure. During the *C*-regime, from 0.76 to 1 ML, (2 2 3) facets develop. With 1 ML we observe a close-packed Ag layer wetting a random distribution of (3 3 5)- and (2 2 3)-like terraces with the same step density as the starting surface.

In the atomic scale, the driving force for the Ag-induced faceting of the stepped Cu surface is the matching between Ag(1 1 1)-like packed rows along the parallel direction of the steps and the Cu facet underneath. Lattice-matching, which lowers the strain contribution to the stress energy [2], has been also proposed as the microscopic mechanism for the NaCl-induced faceting of Cu(1 1 2) [7]. Our system generally displays a clear tendency to avoid adsorption on wide (1 1 1) terraces, which leads to a large mismatch [16]. On the other hand, as deduced from Figs. 1 and 2, there is a preference for (1 1 2)-oriented facets at low coverages, in spite that this requires a larger mass transport. This can be naively explained from the width of the Cu terrace required for a good matching in the perpendicular direction. Five Ag packed rows (2.498 Å wide each) fit to two 6.25 Å wide terraces in Cu(1 1 2) with only 0.12% mismatch in the direction perpendicular to the steps, whereas Cu(3 3 5) requires two 8.37 Å wide terraces to accommodate seven Ag rows with 4.47% mismatch. This prefer-

[2] *A*-regime ideally saturates at 0.61 ML, when Cu stripes become flat (1 1 1) terraces [6]. However some steps appear pinned by defects within Cu stripes, such that the effective saturation coverage is lower.

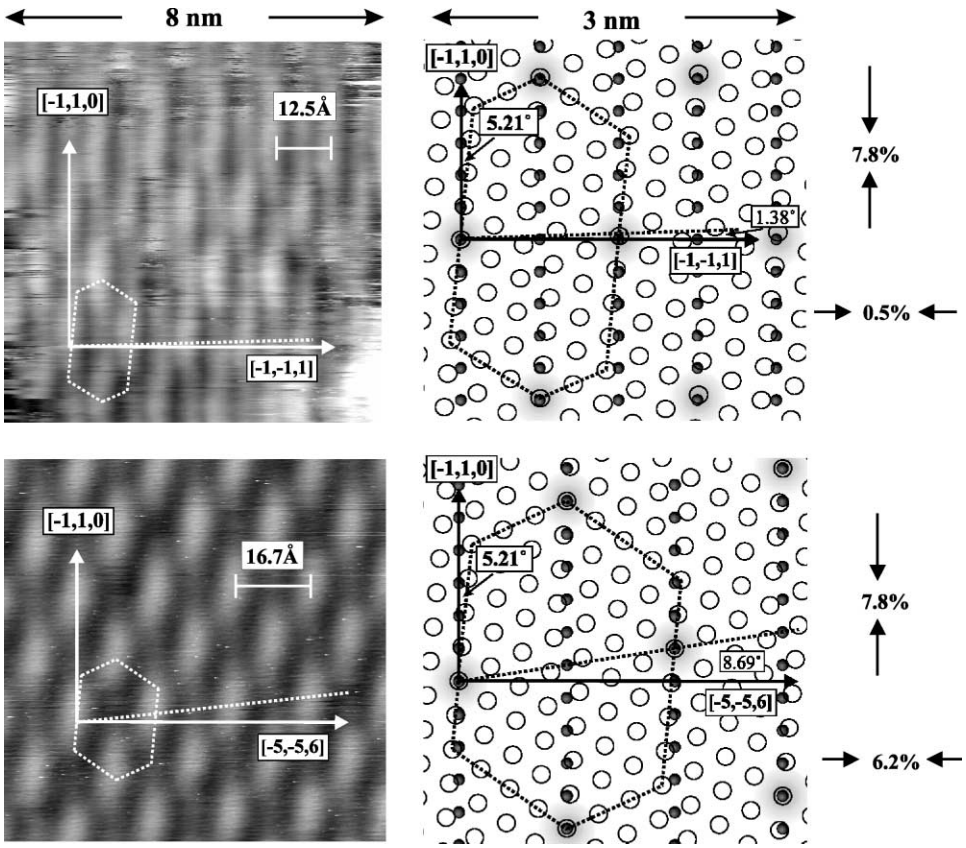

Fig. 3. Left, detailed STM view of the Moiree patterns for (1 1 2) and (3 3 5) Ag-covered facets. Right, two-dimensional atomic models that reproduce the Moirees in the left. The small filled circles indicate the step edge Cu atom positions underneath. Open circles represent Ag atoms and shaded regions indicate "on-top" positions. The fit requires the indicated compressions and azimuthal rotations of the Ag packed layer.

ence for (1 1 2) facets is also supported by the microscopic analysis of (1 1 2) and (3 3 5) stripes shown in Fig. 3. The atomic models in the right panels of Fig. 3 reproduce the Moire patterns of the left panels in the simplest way. The open circles represent Ag-close packed layers, the small dots the Cu(1 1 2) and Cu(3 3 5) unit cell underneath, and the shades the "on-top" positions. Thus, in this simple approach the step corrugation is being disregarded. We use the smallest compressions and azimuthal rotations of the Ag(1 1 1) adlayer to obtain the Moires that fit to the STM observations. For both (1 1 2)- and (3 3 5)-oriented layers the Ag layer rotation is the same 5.2°, allowing the smooth transition from (1 1 2) to (3 3 5) facets observed beyond 0.52 ML. For (1 1 2) facets the Ag adlayer is compressed by 0.5% and 7.8% in the direction perpendicular and parallel to the rows, respectively. For (3 3 5) facets the perpendicular and parallel compressions are 6.2% and 7.8%, respectively. Thus, the (3 3 5)-oriented layer accumulates much more strain, explaining the preference to form (1 1 2)-oriented stripes.

In the following we analyze the long range periodicity of the Ag-induced faceting of Fig. 1. Data points in Fig. 4 represent the nanostructure period L and the Ag stripe width w_{Ag} measured from the STM images as a function of coverage θ from 0.1 to 0.9 ML. The periodicity is poorly defined above 0.52 ML, and in this case we consider the average

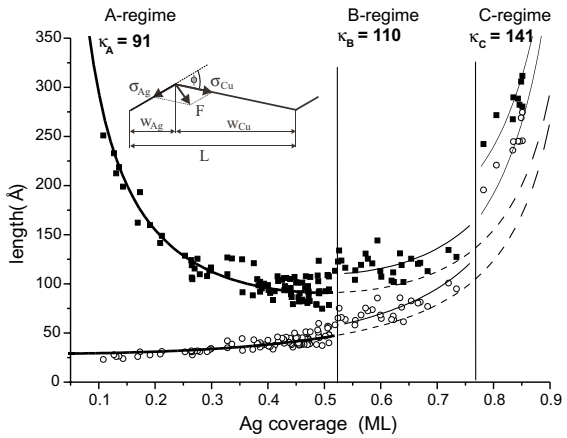

Fig. 4. Nanostructure periodicity (filled squares) and Ag-covered stripe width (open circles) as a function of Ag coverage. Vertical lines distinguish the *A*-, *B*- and *C*-regimes, which differ on the type of the growing Ag-covered facet. The thick solid lines are fit to the data in the two-phase *A*-regime using the continuum elastic theory of Marchenko et al. [9]. A continuation in the *B*- and *C*-regimes is represented by the thin dotted line. The thin solid lines do fit separately data points in the *B*- and *C*-regimes. The inset shows the surface stress vectors in a faceted structure (see the text).

value $\langle L\rangle$, defined as $\langle L\rangle = \langle w_{\mathrm{Ag}}\rangle + \langle w_{\mathrm{Cu}}\rangle$, where $\langle w_{\mathrm{Ag}}\rangle$ and $\langle w_{\mathrm{Cu}}\rangle$, respectively, are the average widths of Ag-covered facets and Cu stripes. Data points at regime transitions display a clear discontinuity. Microscopically, this appears related to the way the new facets develop, i.e., by melting two contiguous Ag-stripes in the previous regime.

Both Cu and Ag stripe widths can be varied smoothly in the 3–30 nm range by tuning Ag coverage. This makes the Ag/Cu(2 2 3) system particularly interesting for a quantitative test of theoretical faceting models. In the simplest approach, the coverage dependent long range periodicity can be explained within Marchenko's elastic theory [9]. The lines in Fig. 4 are fit to the data using Marchenko's model, where the superlattice periodicity L and the stripe width w_{Ag} are given by

$$L(\theta) = \frac{\kappa}{\sin(\pi\theta)}; \quad w_{\mathrm{Ag}}(\theta) = \frac{\kappa\theta}{\sin(\pi\theta)}, \tag{1}$$

κ is the only adjustable parameter. Restricting the fit to the *A*-regime we obtain $\kappa_A = 91 \pm 6$ Å. The fit is excellent, demonstrating that inside this regime the value for κ appears not to depend appreciably on coverage. This gives the evidence that the elastic theory for continuous media is applicable here. As indicated by the dashed lines in Fig. 4, data points at higher coverage regimes cannot be fitted with κ_A. By changing in Eq. (1) to $\kappa_B = 110 \pm 8$ Å and $\kappa_C = 141 \pm 8$ Å both $\langle w_{\mathrm{Ag}}(\theta)\rangle$ and $\langle L(\theta)\rangle$ in *B*- and *C*-regimes one can still obtain a good agreement with Marchenko's model. We conclude that this simple theory is applicable in this system, but with different values of κ in each facet-type regime.

In Marchenko's approach κ is related to elastic constants via:

$$\kappa = 2\pi a \times \exp(1 + C_1/C_2), \tag{2}$$

where a is a characteristic microscopic cut-off of the order of atomic distances and C_1 is the free energy of the phase boundary per unit length [9]. If we assume that work function variations between Cu and Ag phases are relatively small [11], C_2 has only elastic nature and reflects the stress difference between phases [9]: $C_2 = ((1-\nu^2)/\pi E)|\vec{F}|^2$ where E and ν, respectively, are the shear modulus and the Poisson ratio for Cu. In this formula

$$|\vec{F}|^2 = (\vec{\sigma}_{\mathrm{Ag}} - \vec{\sigma}_{\mathrm{Cu}})^2 = \sigma_{\mathrm{Ag}}^2 - 2\sigma_{\mathrm{Ag}}\sigma_{\mathrm{Cu}}\cos\phi + \sigma_{\mathrm{Cu}}^2$$

is the force exerted at facet edges due to the difference in surface stress $\vec{\sigma}$ between Ag-covered facets and Cu stripes and ϕ stands for the angle between adjacent facets, as shown in the inset of Fig. 4. Therefore κ is related to three independent, unknown constants a, C_1, C_2, which in turn cannot be determined from the experiment. Literature values are not available with sufficient accuracy for such complex systems.

Nonetheless it is interesting to discuss the potential influence of the three parameters a, C_1, C_2 on the characteristic lengths assuming the elastic model of Eqs. (1) and (2). First we note that the good fit of Eq. (1) to data points in the *A*-regime discards any remarkable coverage-dependence in κ. Such coverage-dependence is indeed expected for C_2 via changes in σ_{Cu} (changes in $\cos\phi$ are too small). In Au(1 1 1) vicinals [10], the intrinsically stressed (1 1 1) plane is relaxed in the presence of steps, such that σ decreases as a function of $\tan\varphi$,

where φ is the local miscut with respect to the (1 1 1) surface. Assuming the same behavior for Cu(1 1 1), we expect an increase of σ_{Cu} of about 20% as a function of Ag coverage in *A*-regime. In contrast, the structure of the Ag-stripes remains unchanged and hence σ_{Ag} stays constant for *A*-regime. Thus the absence of a coverage dependence suggests the dominant effect of σ_{Ag} ($\sigma_{Ag} \gg \sigma_{Cu}$) in C_2. According to our model in Fig. 3, there is indeed a high stress energy in the Ag-covered facets due to strain, particularly in the direction parallel to the steps where the Ag layer is largely compressed.

In Au(1 1 1) faceting a variety of periodicities are found as a consequence of the delicate balance between the (constant) boundary energy C_1 and the facet-type-dependent C_2 [10]. The boundary energy in that case is of the order of the step energy, which displays minor variations for all noble metal surfaces [18]. In our Ag-induced faceting, C_1 can be assumed to be the energy needed to add or remove a Ag(1 1 1) atomic row, i.e., also of the order of the Ag(1 1 1) step energy. But in our case, since C_2 appears to be determined by a high σ_{Ag}, the boundary energy will surely be unbalanced by the stress constant C_2. Therefore, despite that the stress situation must be different for all three regimes, we expect $C_1/C_2 \sim 0$ in the whole coverage range due to the high stress of the Ag-covered facets.

Note that if $C_1/C_2 \sim 0$ in Fig. 4, the changes in κ at different regimes must be mostly explained by changes in the cut-off length a. The physical nature of a is not clear in elastic theory. Although it appears as an artificial way of avoiding divergence in energy integrals [9], it should be understood as the minimum size of the domains, from which one has to integrate [11]. For clean, non-reconstructed surfaces the natural choice of a is thus the atomic row distance in terraces [10]. In vicinal Si(1 1 1) the facet width is a multiple of the (7×7) unit cell, which thereby defines the cut-off length [17].

Following these arguments, in Ag/Cu faceting one can take the cut-off length as the minimum size of the (growing) Ag-covered facet, i.e., the terrace width underneath. This is indeed supported by a close evaluation of STM topographs, which clearly show Ag-stripes growing laterally by multiples of the terrace width d of the underlying Cu-facet, i.e., $d_{112} = 6.25$ Å, $d_{335} = 8.4$ Å, and $d_{223} = 10.5$ Å at *A*-, *B*- and *C*-regimes, respectively. Assuming $C_1/C_2 = 0$ in Eq. (2) and using the different values of κ obtained in the separate fits in Fig. 4, we obtain $a_{112} = 5.3$ Å, $a_{335} = 6.4$ Å, and $a_{223} = 8.3$ Å. The order of magnitude and the growing trend is correct, although the absolute numbers still fall 15–25% short with respect to the terrace width.

On the other hand, assuming a constant cut-off length of the order of the atomic distances in the whole coverage, the discontinuities of Fig. 4 would indicate that C_1/C_2 increases from *A*- to *B*- and *C*-regimes. This is unlikely. The boundary energy C_1 must be very similar in the three regimes, because the atomic structure at facet edges, as observed in the STM figures or deduced from the Moire analysis in Fig. 3, is the same. Thus the different κ values in the separate fits would indicate that $C_2^{(112)} > C_2^{(335)} > C_2^{(223)}$, in contrast with the observation of a preferred (less stressed) (1 1 2)-faceting at early coverage.

Note that the $C_1/C_2 \sim 0$ case leads to the shortest possible superlattice period in Ag/v-Cu(1 1 1). This contrasts with the long superlattice periods observed at high temperatures in NaCl/v-Cu(1 1 1) [7]. Long periods are only possible if $C_1/C_2 \gg 1$, which in the latter case could be due to a more efficient interface relaxation, favored by a large adsorbate-surface charge transfer that weakens Cu–Cu bonds.

In summary, the driving forces for Ag induces periodic faceting of v-Cu(1 1 1) have been studied with STM. At the atomic scale, this phenomenon is explained by lattice matching Ag packed rows with different Cu facets. In the mesoscopic scale, despite the general complexity of the system, the characteristic lengths are well explained using Marchenko's elastic theory at thermal equilibrium. We observe coverage-dependent discontinuities of the faceting periodicity related to the successive appearance of different Ag-covered facet orientations. A semi-quantitative analysis within Marchenko's model indicates a high stress energy in Ag-covered facets and a different cut-off length at different facet-type regimes. The latter appears as an interesting issue that deserves a more refined microscopic model.

Acknowledgements

A.R.B. and S.S. are supported by the Stichting voor Fundamenteel Onderzoek der Materie (FOM) and the Deutsche Forschungsgemeinschaft (DFG). A.M. and J.E.O. are supported by the Universidad del País Vasco (1/UPV/EHU/00057.240-EA-8078/2000) and the Max Planck Research Award Program. Fruitful discussions with A. Rubio are acknowledged.

References

[1] J. Hannon et al., Science 295 (2002) 299; R. Plass et al., Nature 412 (2001) 875.
[2] V.A. Shchukin et al., Rev. Mod. Phys. 71 (1999) 1125; H. Ibach, Surf. Sci. Rep. 29 (1997) 195.
[3] L. Seehofer et al., Surf. Sci. 329 (1995) 157; K. Aoki et al., Surf. Sci. 408 (1998) 101; H. Minoda et al., Surf. Sci. 432 (1999) 69.
[4] F.J. Himpsel et al., J. Phys. Condens. Matter 13 (2001) 1.
[5] H. Minoda et al., Phys. Rev. B 59 (1999) 2363; M. Horn von Hoegen et al., Surf. Sci. 433–435 (1999) 475.
[6] A.R. Bachmann et al., Phys. Rev. B 64 (2001) 153409.
[7] S. Fölsch et al., Phys. Rev. Lett. 84 (2000) 123; S. Fölsch et al., Surf. Sci. 497 (2002) 113.
[8] C.H. Nien et al., Phys. Rev. B 59 (1999) 10335; T.E. Maday et al., Surf. Rev. Lett. 3 (1996) 1315.
[9] V.I. Marchenko et al., Sov. Phys. JETP 52 (1980) 129.
[10] S. Rousset et al., Surf. Sci. 422 (1999) 33.
[11] D. Vanderbilt, Surf. Sci. 268 (1992) L300; K.-O Ng et al., Phys. Rev. B 52 (1995) 2177.
[12] J. Tersoff et al., Phys. Rev. Lett. 75 (1995) 2730; F. Liu et al., Phys. Rev. Lett. 80 (1998) 1268.
[13] F.-J. Meyer zu Heringdorf et al., Phys. Rev. Lett. 86 (2001) 5088.
[14] M. Henzler, Appl. Phys. A 9 (1976) 11.
[15] A.R. Bachmann et al., to be published.
[16] I. Meunier et al., Phys. Rev. B 59 (1999) 10910.
[17] F.K. Men et al., Phys. Rev. Lett. 88 (2002) 96105.
[18] M. Giesen, Prog. Surf. Sci. 68 (2001) 1–154.